

EXPERIMENTALLY PRODUCED SPINEL RIMS ON Ca-AL-RICH INCLUSION BULK COMPOSITIONS. J. M. Paque¹, L. Le², G. E. Lofgren³, ¹SETI Institute, NASA-Ames Research Center, M. S. 245-3, Moffett Field, CA 94035-1000, julie@paque.org, ²Lockheed-Martin, 2400 NASA Road 1, Houston, TX, 77058, loan.le1@jsc.nasa.gov, ³SN-4, NASA-JSC, Houston, TX, 77058, gary.e.lofgren1@jsc.nasa.gov.

Most Ca-Al-rich inclusions (CAIs) from Allende are surrounded by a series of mineralogically distinct rim layers [1]. Proposed modes of formation for these layers include flash heating, evaporation, and condensation (see summary in [2]). The innermost of these rim layers is generally spinel (SP), in some cases intergrown with perovskite (PV), and commonly containing varying amounts of secondary iron increasing towards the edge of the CAI. The SP or SP+PV rim is not always contiguous with the other rim layers, indicating that it is probably the result of a separate event. We have produced continuous SP rims on synthetic analogs representing Type A/B1, average Type B, and Type B2 bulk compositions by reheating a solid glass experimental charge to subliquidus crystallization temperatures.

This experimental result is consistent with the formation of chondrules and CAIs by more than one sequence of heating and cooling [3, 4, 5]. Previous work [6] indicated that prior crystallization events produced observable effects in the texture and chemistry of the final run product. Information on the nature of the heating/cooling cycles experienced by CAIs and chondrules is important in modeling the environment of their formation.

Experimental Techniques. Four starting materials, representing a wide range of CAI compositions, were used (Table 1). Isothermal crystallization sequences and preliminary controlled cooling experimental results can be found in [7]. Under isothermal conditions SP is the liquidus phase for all bulk compositions except TCAN (Type C analog), which has anorthite (AN) as the liquidus phase. The starting materials were prepared as previously described [8, 9]. The experiments were carried out in air in a vertical tube Deltech furnace. Cooling rates were controlled with a Eurotherm programmer and samples were quenched in air.

Table 1. Compositions of starting materials (wt. %).

start. material	CAI	B2C	98	TCAN
inclusion type represented	avg. Type B	Type B2	Type A/B1	Type C
SiO ₂	31.1	35.7	25.8	38.8
TiO ₂	1.12	1.39	1.51	1.31
Al ₂ O ₃	28.3	27.1	32.6	29.0
MgO	10.1	12.9	6.65	5.77
CaO	29.2	22.4	33.7	24.9
Total	99.8	99.5	100.2	99.7
liquidus T (°C)	1550	1545	1540	1400
1 st stage melting T (°C)	1580	1560	1550	1450

For the two stage experiments the finely ground glass powder was attached to a Pt hanging wire with polyvinyl alcohol. The furnace was brought to a temperature above the liquidus (see 1st stage melting T in Table 1) and the

sample was placed in the furnace for 1 hour and quenched in air. A representative run product from the 1st stage for each bulk composition was examined optically and by backscatter electron imaging to ensure that the charge was totally glass. For the second stage of the experiments the furnace was brought to a run temperature (T_{max}) below the liquidus. The totally glass charge was reinserted into the furnace, and as soon as the sample reached the run temperature, was cooled at 20°C/hr to a temperature below 1000°C.

Several additional experiments were run on the CAI analog to determine exactly when the SP rim was forming. For these runs a totally glass charge was formed in the same manner as described above. Then the furnace was set to T_{max} (varied between 1420 and 1500°C), but the sample was removed from the furnace before the reference thermocouple reached the run temperature. The sample was in the furnace for no more than a few minutes for these experiments.

Experiments were also performed by bringing a powdered sample to the 1st stage melting temperature and holding for one hour, then immediately cooling the furnace to the run temperature (without removing the sample), followed by cooling at 20°C/hr to a temperature below 1000°C. SP rims were not produced in any experiments under these conditions.

Polished sections were made of the run products, which were examined by reflected light microscopy, backscatter electron imaging, and analyzed for major element composition by electron microprobe.

Results. Continuous SP rims (Figure 1) were produced on the surfaces of the experimental charge for the two stage experiments on the CAI, B2C, and 98 bulk compositions. The thickness of the SP rim increases as T_{max} increases, and varies from 5 μ m to 45 μ m (Table 2). As the thickness of the SP rim increases the amount of SP in the interior of the experimental charge decreases. SP also forms around the Pt hanging wire in all experiments.

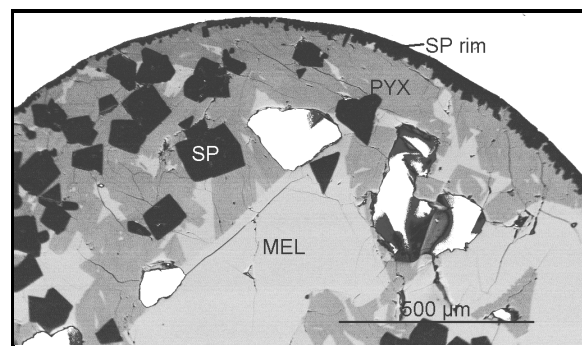


Figure 1. Backscatter electron image of spinel rim from a CAI analog ($T_{max}=1420^{\circ}\text{C}$). The white areas are holes. SP=spinel; MEL=melilite; PYX=pyroxene. The scale bar in the lower right is 500 μ m long.

SPINEL RIMMING OF CAIs: J. M. Paque, *et al.*

The overall texture of the spinel, melilite, and pyroxene in the $T_{\max}=1420^{\circ}\text{C}$ experiment on the CAI bulk composition is similar to Allende CAIs. Experiments on the 98 bulk composition were finer grained than their natural counterparts, suggesting a T_{\max} higher than 1500°C would be appropriate.

The TCAN bulk composition (Type C analog) did not produce spinel rims, and is also the only bulk composition that does not have spinel as the liquidus phase. Natural Type C CAIs generally have no rim or a very narrow rim sequence [10].

Table 2. Thickness of the spinel rim as a function of 2nd stage T_{\max} .

T_{\max} ($^{\circ}\text{C}$)	CAI	B2C	98	TCAN
1500	45 μm		15 μm	
1450	25 μm		10 μm	
1420	25 μm		10 μm	none
1400		10 μm	5 μm	none
1380				none
1360				none
1350		10 μm		
1300		5 μm		

Experiments quenched as the sample was heating to run temperature suggest that spinel crystallizes as the sample is heating. Figure 2 shows a spinel rim on the surface of a glass charge produced by inserting a glass charge of the CAI bulk composition into a furnace set at 1500°C . The sample was removed from the furnace when the adjacent thermocouple recorded 1300°C (i. e., before the sample equilibrated with the furnace temperature).

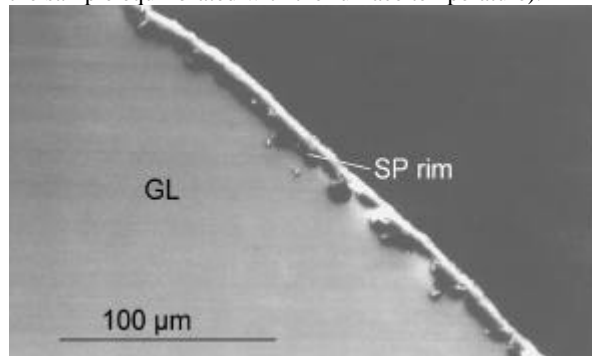


Figure 2. Backscatter electron image of spinel rim formed during heating of experimental charge. GL=glass.

Discussion and Summary. The production of spinel rims on experimental analogs to CAIs has important implications for both the formation of SP rims on natural CAIs and SP palisades [11, 12].

The process by which SP rims form on CAIs in experiments requires starting material free of nucleation sites, and relies on surface nucleation (e.g., dust). SP nucleates on the surface of the experimental charge as the sample is heating up to the maximum temperature, but only if the starting material is solid glass. With crystallized or powdered glass starting material, SP crystallizes throughout the sample [6]. This suggests that at some point in the history of CAIs (containing SP rims)

they were quenched to a glass and then reheated (perhaps more than once) to a temperature below their liquidus.

SP palisades have been proposed to be a result of direct condensation from the vapor phase [11], incorporation of earlier formed CAIs [12], or in situ formation during crystallization of the CAI [13]. Figure 3 illustrates the spinel texture formed when nucleation occurs on the surface of the object. Note the smooth alignment of spinels along the convex outer surface. This is the most common texture found in palisade bodies (e.g., Fig. 1b of [13]). On the other hand, nucleation on the surface of gas bubbles within the sample produces a ring of spinels with alignment along a concave surface (e.g., Fig. 2c of [13]). This argues against the formation of palisade bodies by direct crystallization with the CAI as proposed by [13].

Incorporation of earlier formed CAIs [12] could easily produce the spinel palisade textures, provided the conditions necessary for SP rim growth were experienced by the incorporated CAI. Repeated heating events account for the lack of sphericity seen in many palisades. Partial melting could homogenize the melt in the incorporated CAI with the remainder of the inclusion.

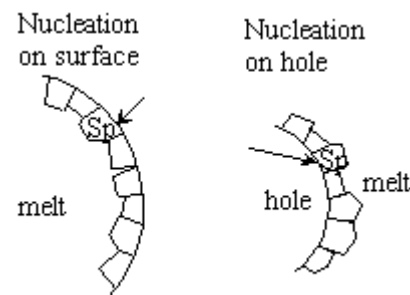


Figure 3. Nucleation on surface of sample causes alignment along a convex surface. Nucleation on a hole or void within the sample creates alignment along a concave surface.

References. [1] Wark D. A. and Lovering J. F. (1977) Proc. LPSC 8th, 95-112. [2] Murrell M. T. and Burnett D. S. (1987) *Geochim. Cosmochim. Acta*, **51**, 985-999. [3] Wasson J. T. (1993) *Meteoritics*, **28**, 14-28. [4] Jones R. H. (1996) in *Chondrules and the Protoplanetary Disk* (Eds., R. H. Hewins, *et al.*), 163-172. [5] Rubin A. E. and Krot A. N. (1996) in *Chondrules and the Protoplanetary Disk* (Eds., R. H. Hewins, *et al.*), 173-180. [6] Paque J. M., Le L. and Lofgren G. E. (1997) *LPSC XXVII*, 1073-1074. [7] Paque J. M. and Stolper E. (1984) *LPSC XV*, 631-632. [8] Stolper E. (1982) *Geochim. Cosmochim. Acta*, **46**, 2159-2180. [9] Stolper E. and Paque J. M. (1986) *Geochim. Cosmochim. Acta*, **50**, 1785-1806. [10] Wark D. A. (1987) *Geochim. Cosmochim. Acta*, **51**, 221-224. [11] El Goresy A., Nagel K. and Ramdohr P. (1979) Proc. LPSC 10th, 833-850. [12] Wark D. A. and Lovering J. F. (1982) *Geochim. Cosmochim. Acta*, **46**, 2595-2607. [13] Simon S. B. and Grossman L. (1997) *Meteoritics and Planet. Sci.* **32**, 61-70.